Glass Transition in Polymer Melts: Study of Chain-Length Effects by Monte Carlo Simulation

B. Lobe, J. Baschnagel,* and K. Binder

Institut für Physik, Johannes-Gutenberg Universität, 55099 Mainz, Germany

Received January 18, 1994; Revised Manuscript Received April 25, 1994®

ABSTRACT: This paper presents results of a Monte Carlo simulation for the glass transition in a three-dimensional polymer melt. The melt was simulated by the bond-fluctuation model on a simple cubic lattice, which was amended by a two-level Hamiltonian favoring long bonds in order to generate a competition between the energetic constraints and the density of the melt. The development of this competition during the cooling process makes the melt adopt configurations, from which it cannot easily relax, and thus facilitates the freezing of the melt in an amorphous structure, as soon as the internal relaxation times match the observation time of the simulation set by the cooling rate. How pronounced the effects of this competition are depends upon the chain length, whose influence on the vitrification process we want to study by monitoring various quantities that probe different length scales of a polymer, such as the mean bond length or the radius of gyration. As the melt vitrifies, these quantities gradually become independent of temperature, and their value at low temperatures is strongly influenced by the chain length. This influence qualitatively resembles that of a variation of the cooling rate. The larger the chain length (cooling rate), the faster the various quantities fall out of equilibrium, and the earlier the melt freezes on the corresponding length scale. It is thus possible to infer from these quantities the chain-length dependence of the glass transition temperature T_g. This analysis shows that T_g approximately increases linearly with the inverse chain length.

I. Introduction

If one cools a liquid, it usually crystallizes at its melting point unless one performs the cooling very rapidly so that crystallization nuclei can neither be created nor grow sufficiently.[1,2] By rapid cooling one may thus undercool the liquid and keep it in the amorphous state until finally a temperature is reached, where the viscosity η has become so large that the dynamical behavior of the liquid can no longer be distinguished from that of a solid on the time scale of the experiment.[1,2] Then the liquid freezes in an amorphous disordered state; i.e., it vitrifies. Therefore, the temperature, corresponding to this viscosity which is typically on the order of $\eta = 10^{13}$ P, has been defined as the glass transition temperature T_g. Which cooling rate must be used to bypass crystallization and to form a glass depends upon the nature of the liquid. Metallic alloys, for instance, possess a high tendency to crystallize. Cooling rates up to 10^8 K s^{-1} are needed to vitrify them.[2] Contrary to that, the crystalline state is rather an exception for polymeric materials. They prefer to remain in the amorphous state, even if they are cooled very slowly. Typical cooling rates range between 10^{-4} and 10^{-1} K s^{-1},[2] which already comes close to a quasi-static and thus thermodynamically well-defined cooling process. Due to this ease to vitrify a polymer melt, an important aspect of polymer physics is to elaborate the microscopic properties of the chains, which essentially influence the glass transition, and to establish relationships between them and macroscopic quantities, such as the glass transition temperature. From experiments on aromatic vinyl polymers, for instance, one can infer that the glass transition temperature increases if the backbone of the chains stiffens.[3] This observation may be rationalized by the physical perception that the glass transition happens in the melt as soon as the polymers build up spatial obstacles that mutually hinder the motion of the chains. The stiffer parts of the chains are, the larger voids are required to enable a reorientation of the corresponding segment and thus the more the mobility of the chains is reduced, resulting in a shift of T_g to larger temperatures.[3] Hence, the observed relationship of the glass transition temperature and the flexibility of the polymers may be explained by rather general ideas about the impact of microscopic properties on the macroscopic behavior of the melt, which should not be limited to aromatic vinyl polymers but apply to other classes of polymeric materials as well. By these general considerations, it is certainly not possible to make quantitative predictions for a specific polymer, but qualitative trends may be understood or even predicted.

Being primarily interested in these qualitative aspects of the glass transition in polymer melts, one may thus work with microscopically unrealistic, coarse-grained models which only retain the essential features of a polymer melt, such as chain connectivity and self-avoidance of the chains.[4] Such coarse-grained models have extensively been used in both analytical[5] and computer studies[4] of polymer properties. For computer simulations lattice models are especially appealing since they can be simulated very efficiently. Good statistics and the observation of slow relaxation processes being characteristic of the glass transition are thus accessible. Such a lattice model for dense polymer melts is the bond-fluctuation model.[6] Combining the model with a Hamiltonian which associates an energy with the bond length, many experimental features of the glass transition may be reproduced.[7-10] If one cools the melt, its structural relaxation time strongly increases, the temperature dependence of which may be fitted to a Vogel-Fulcher equation.[8,9] As soon as the structural relaxation time becomes comparable to the time scale of the simulation, set by the cooling rate, the melt freezes in an amorphous liquidlike structure.[10] Close to this freezing point all static quantities, such as the glass transition temperature, for instance, become cooling rate dependent. If one extracts this dependence from the simulation data, one obtains a nonlinear relationship between the glass transition temperature and the logarithm of the cooling rate, which may be described by a variation of the Vogel-Fulcher equation.[9] These latter results concerning the cooling rate dependence were also found in a recent experiment.[11]

* To whom correspondence should be addressed.

® Abstract published in *Advance ACS Abstracts*, June 1, 1994.

0024-9297/94/2227-3658$04.50/0

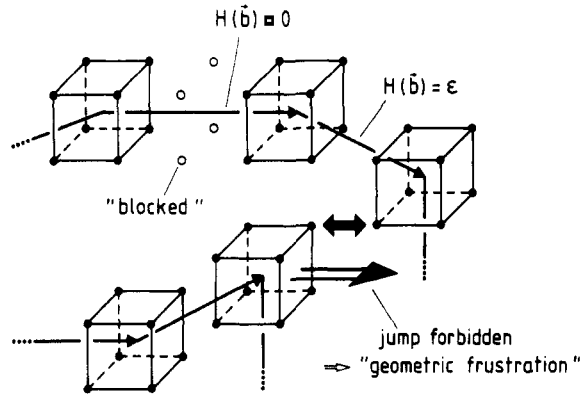

Figure 1. Sketch of a possible configuration of monomers belonging to different chains in the melt in order to illustrate the effect of the Hamiltonian and the concept of geometric frustration. All bond vectors have the energy ϵ except the vector (3,0,0) which belongs to the ground state. This vector blocks four lattice sites (marked by O) which are no longer available to other monomers since two monomers may not overlap. Due to this self-avoiding walk condition, the jump in the direction of the large arrow is also forbidden. If a monomer tried to reach the ground state (i.e., a bond vector from the class [3,0,0]) by such a jump, the presence of the monomer in its surroundings would prevent this trial (geometric frustration).

In this paper we want to extend the analysis by studying the influence of the chain length on the glass transition and on the structure of the frozen state in this model. The content of the subsequent sections deals with the following topics: First, we briefly review the essential aspects of our model and give some details about the simulation procedure in section II. Section III presents the influence of the chain length on the freezing behavior of the melt, which we exemplify by several quantities being sensitive to different length scales of the polymers. Section IV is devoted to the discussion of the chain length dependence of the glass transition temperature, and the final section V summarizes our main results and presents a brief outlook on future work.

II. Basics of the Model and the Simulation

The polymers of the bond-fluctuation model[6] are self-avoiding and mutually avoiding walks on a simple cubic lattice, where each monomer corresponds to a whole unit cell of the lattice. The bond vectors $\vec{b}$ between the monomer n and $n+1$ of polymer p in configuration c are chosen in such a way that the chains are self-avoiding and cannot cross each other during the course of their motion on the lattice.[6] In order to introduce the temperature in this *a priori* athermal model, long bonds with a length of 3 and direction along the lattice axes, i.e., $\vec{b} \in [3,0,0]$, are favored in comparison to all other available bond vectors:

$$\mathcal{H}(\vec{b}) = \begin{cases} 0 & \text{if } \vec{b} \in [3,0,0] \\ \epsilon & \text{else} \end{cases} \qquad (1)$$

The effect of this Hamiltonian is that a bond in the ground state blocks four lattice sites which are no longer accessible for other monomers due to the self-avoidance condition. This loss of available volume results in a competition between the bond energy and the density of the melt so that some bonds are forced to remain in the excited state (see Figure 1). They are *geometrically frustrated*.[9,10] In order to generate this geometric frustration which facilitates the maintenance of the amorphous structure of the melt during the cooling process,[9] the density of the melt has to be chosen suitably. A possible choice for the density is $\phi = 0.5\bar{3}$.[9,10]

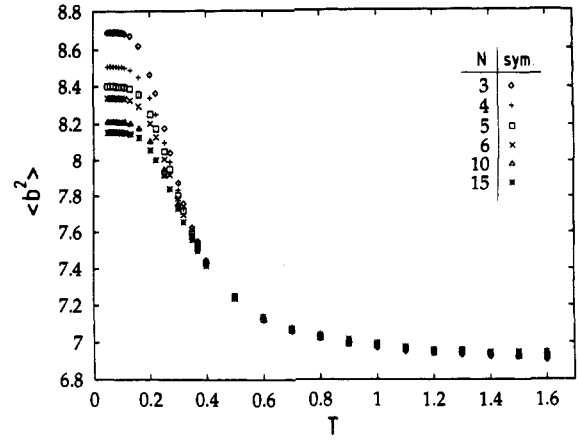

Figure 2. Plot of the mean-square bond length versus T for six representative chain lengths N: 3 (◇), 4 (+), 5 (□), 6 (×), 10 (△), 15 (*). The cooling rate is $\Gamma_Q = 4 \times 10^{-6}$. The error bars are of the size of the symbols and therefore omitted.

The simulation is started from well-equilibrated configurations at infinite temperature, which contain polymers having a chain length N between $N = 3$ and $N = 15$. Note that each effective monomer of our model can be interpreted—at least roughly—as a group of three to five chemical monomers along the backbone of a chain.[7,9] Thus our study physically corresponds to very short chains with a degree of polymerization N_p from about $N_p \approx 12$ to 60. The melt is cooled by continuously lowering the reciprocal temperature β according to the following cooling schedule:[9,10]

$$\beta = \beta_{max}\Gamma_Q t \qquad (2)$$

In this equation β_{max} and Γ_Q stand for the smallest temperature, where the cooling is stopped, i.e., for $\beta_{max} = 1/T_{min} = 20$, and for the cooling rate, respectively. Since the results for various cooling rates turned out to behave qualitatively in the same way and since the influence of the cooling rate on the freezing behavior of the melt was investigated before,[9,10] we used the fastest cooling rate, i.e., $\Gamma_Q = 4 \times 10^{-5}$,[12] of our previous study[9,10] in this work, for which data accumulation is fastest and thus good statistics may be obtained. With this cooling rate it was possible to run 160 independent configurations from which each comprised 1800 monomers. Therefore, our total statistical effort is based on 288 000 monomers. Combining this with an error analysis that takes correlations into account,[13] the statistical inaccuracy is well under control in this simulation. If not stated explicitly, the errors are always either smaller or of the size of the symbols in subsequent sections.

III. Influence of the Chain Length

A deeper insight into the influence of the chain length on the structural properties of the melt may be obtained if one monitors the temperature dependence of quantities that probe different length scales in the system. *A priori*, there are two relevant length scales in a melt: the scale of the bond and that of the radius of gyration. Quantities sensitive to changes on these scales are, for instance, the mean-square bond length and the radius of gyration itself. They will be discussed in the next subsection.

A. Mean-Square Bond Length and Radius of Gyration. The temperature dependence of the mean-squared bond length $\langle b^2 \rangle$ for six representative chain lengths, i.e., $N = 3, 4, 5, 6, 10, 15$, is depicted in Figure 2. In the high-temperature region ($T \in [0.6, 1.6]$) the curves for the different chain lengths nicely collapse, indicating

that the melt is thermally equilibrated. In this state the polymers, irrespective of their length, are mobile enough to adapt to the speed by which the temperature is changed. Their structural relaxation time on the length scale of a bond is thus significantly smaller than the time scale defined by the cooling rate. Therefore, the bond length increases only by about 4% in this temperature region, although many bonds—to be more precise, about 15%—reach the ground state, as can be inferred from the mean energy per bond (not shown here), for instance. This observation about the influence of the chain length on the temperature dependence of the length scale of a bond vector exactly corresponds to the effects of the cooling rate on the same length scale, described in ref 9, and it may thus be rationalized in a similar fashion: As stated in the previous section, a bond in the ground state blocks four lattice sites for further occupancy by other monomers. This reduction of available volume has to be compensated by a corresponding shrinking of other bond vectors in order to keep the density constant. However, the compensation can only take place if the melt has enough time to overcome the free energy barriers at the respective temperature. It is certainly possible in the high-temperature region, whereas it becomes progressively more difficult for lower temperatures. Therefore, the bond length strongly increases if the temperature is decreased below $T \approx 0.5$. This increase stops at a temperature at which the structural relaxation time on the length scale of a bond becomes comparable to the time scale of the simulation. Then the melt fully falls out of equilibrium on this length scale, and the mean-square bond length gets arrested at a temperature-independent, but chain-length dependent, value. This constant value for $\langle b^2 \rangle$ in the glassy phase increases with decreasing the chain length. However, for all chain lengths it is smaller than 9, i.e., than the value expected if all bonds were in the ground state, which indicates that many bonds are geometrically frustrated. Therefore, the melt is frozen in an amorphous structure on the time scale of the simulation for temperatures smaller than $T \approx 0.1$, and the corresponding low-temperature region ($T \in [0.05, 0.1]$) will be called the "glassy phase". This influence of the chain length, which becomes clearly visible in the glassy phase, already gradually develops in the intermediate-temperature region, i.e., for $T \in [0.2, 0.5]$, where the curves for the different N start to splay out, and may be explained in the following way: Since chain ends possess a higher mobility than inner monomers,[14,15] the overall ability of a polymer to relax will enhance the smaller the polymer is. Therefore, small chains may approach the ground state more closely than long chains if the cooling is done by a finite rate. As soon as the associated cooling time compares in size to the relaxation time of a chain in the melt, the global structure of the polymer starts to freeze, the effects of which should quickly spread down to the smallest length scales of the polymer due to the building up of spatial constraints by the interplay of the chain connectivity with the density of the melt. Because of this coupling of the global and the local relaxation ability, one might therefore anticipate the observed influence of the chain length of the state of the bond if the temperature is not reduced quasi-statically.

With this interpretation in mind, it is thus interesting to see how the radius of gyration R_G^2 behaves during the cooling process. The result of the simulation is shown in Figure 3 where the ratio of the radius of gyration and the number of bonds is plotted versus temperature for the same six representative chain lengths as in Figure 2. This ratio was chosen for the ordinate because one expects the

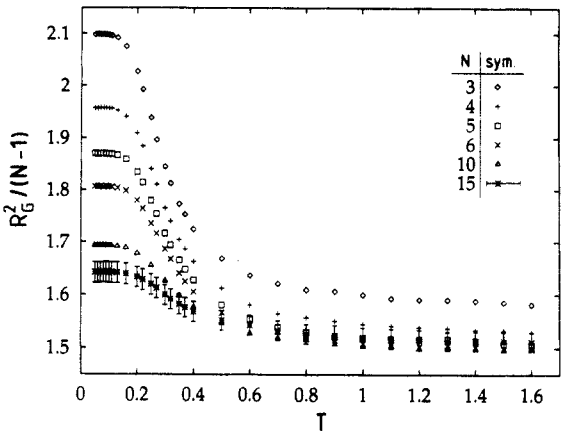

Figure 3. Plot of the ratio $R_G^2/(N-1)$ versus T for the same chain lengths and cooling rate as in Figure 2. The error bars are only shown for $N = 15$ for the sake of clearness. Since the number of chains increases with decreasing chain length in this simulation, the error bars for $N < 15$ are smaller than those for $N = 15$.

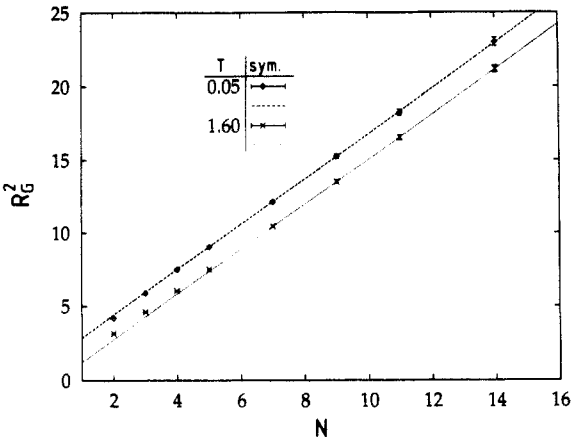

Figure 4. Variation of R_G^2 with the number of bonds for a temperature from the glassy region (i.e., $T = 0.05$ (◇)) and from the equilibrium liquid (i.e., $T = 1.6$ (×)) region.

polymers of a thermally equilibrated melt to exhibit mean-field behavior, i.e., $R_G^2 \propto N - 1$, for large N.[5] How large the chains have to be in order to fulfill this expectation depends upon the studied model. A glance at Figure 3 shows that the bond-fluctuation model seems to reach the limiting mean-field behavior in the high-temperature region already if $N \geq 5$. Only the smallest studied chain lengths $N = 3$, 4 deviate from it, as can also be seen from Figure 4. Besides this expected different dependence on the chain lengths in the high-temperature region, the behavior of the radius of gyration during the cooling process is similar to that of the mean-square bond length. Following the high-temperature region, where the chains extend only very slightly, R_G^2 steeply increases for temperatures below $T \approx 0.5$, before it crosses over to a constant, chain-length-dependent value when the melt vitrifies. As for $\langle b^2 \rangle$, this final frozen-in value of R_G^2 is larger, the smaller the chain length is, emphasizing again the important contribution of the more mobile chain ends to the ability of the chains to relax. This effect of the chain ends is also visible in Figure 4, where the N-dependence of R_G^2 for a typical temperature from the glassy region (i.e., for $T = 0.05$) is compared to one of the equilibrated liquid, i.e., to $T = 1.6$. If the large chains could be kept in thermal equilibrium during the cooling process, one would expect them to stiffen with falling temperature.[5,16] Resulting from this stiffening, the slope of the linear relationship between R_G^0 and N should increase, on the other hand, and, on the other hand, the limiting mean-field behavior should be adopted later.[16]

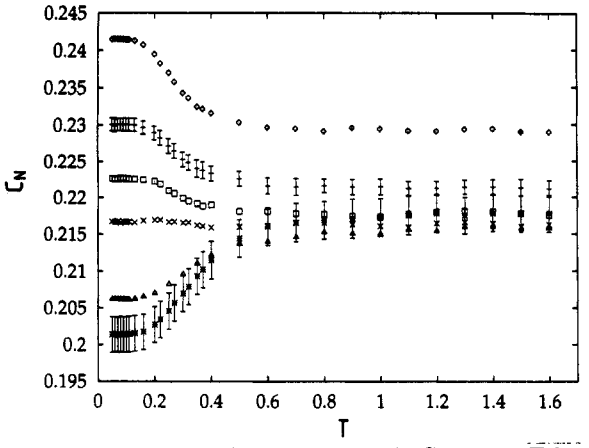

Figure 5. Plot of the characteristic ratio C_N versus T for the same chain lengths and cooling rate as in Figure 2. The symbols in the figure correspond to the following chain lengths N: 3 (◇), 4 (+), 5 (□), 6 (×), 10 (△), 15 (*). The cooling rate is $\Gamma_Q = 4 \times 10^{-5}$. The error bars are only shown for $N = 4$, 15 for the sake of clearness.

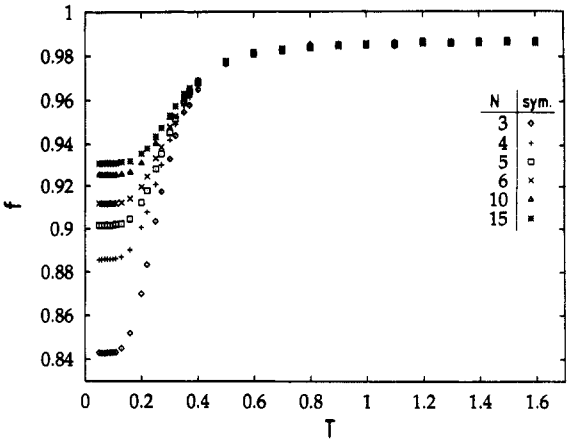

Figure 6. Flory parameter f vs T for the same chain lengths and cooling rate as in Figure 2. The errors are of the same size as for $\langle b^2 \rangle$.

Contrary to these expectations, Figure 4 shows that the low-temperature data for large N are essentially shifted parallel to higher values of R_G^2 in comparison to the results at $T = 1.6$. Only for small chains are there distinct qualitative differences between $T = 0.05$ and $T = 1.6$. Whereas the high-temperature data lie above the asymptotic mean-field behavior, as expected in thermal equilibrium,[16] the quenched results for the small chain lengths at $T = 0.05$ bend downward and finally fall below the straight line for $N = 3$. This opposite curvature of the low-temperature R_G^2 vs N curve compared to that at high temperatures is just another facet of the fact that large chains cannot expand as strongly as small chains during the finite cooling process. Therefore, the slope of the asymptotic mean-field behavior does not enlarge sufficiently to keep the result for $N = 3$, 4 lying above it. Nevertheless, the fact that the mean-field behavior may also be observed for $T = 0.05$ proves that the chains maintain their Gaussian structure[5] that they have a higher and intermediate temperatures, while undergoing the glass transition, a result which was also borne out by an analysis of the chain's structure factor.[10]

Despite the mentioned qualitative similarities between the behavior of $\langle b^2 \rangle$ and R_G^2, a closer comparison of the two quantities reveals that the chain length affects the strength of stretching on the two length scales quite differently. For $N = 3$ R_G^2 expands faster than $\langle b^2 \rangle$, whereas the opposite is true for $N = 15$. This conclusion drawn from Figures 2 and 3 should become better visible if one plots the characteristic $C_N := R_G^2/(N-1)\langle b^2 \rangle$[17] versus temperature for the different chain lengths. This is done in Figure 5. Indeed, the mean-square bond length expands faster than the radius of gyration if the chain length is large. This observation may again be rationalized in terms of length-scale-dependent relaxation times of the polymers: From the theory on the polymer dynamics[5] it is known that the relaxation time increases with the length scale along the chain. Therefore, the radius of gyration relaxes much more slowly than the bond length for large chains. Since the cooling is done with a finite speed, the radius of gyration feels the finiteness of the cooling rate at a higher temperature than the bond length which might still expand, whereas R_G^2 is already essentially frozen. If one also wants the radius of gyration to relax further, one has to decrease either the chain length for fixed cooling rate or the cooling rate for fixed chain length.[9] Hence, chain length and cooling rate qualitatively affect the structure of the chains in the same way, while the melt falls out of equilibrium and undergoes the glass transition.

B. Mean Bond Angle and Flory Parameter. Since the Hamiltonian of this model only associates an energy with the bond length and thus does not directly influence the orientation of the bond vectors, it is interesting to see how correlations between adjacent bond vectors develop with falling temperature as a result of the interplay between this Hamiltonian and the density. That these correlations have to be present may be inferred from the discussion of the previous subsection. The radius of gyration is only able to expand stronger than the mean-square bond length if the bond angles also increase on the average. Therefore, we want to look more closely at the temperature and chain-length dependence of the mean bond angle and of a related quantity, the Flory parameter, in this subsection.

By the Flory parameter we mean the probability of a bond angle to differ from 180°, i.e.

$$f(T) := 1 - P(\vartheta, T)|_{\vartheta=180°} \tag{3}$$

where $P(\vartheta, T)$ represents the probability for the bond angle ϑ to occur at temperature T.[9] Figure 6 presents a plot of this parameter versus temperature for the six representative chain lengths. Although the temperature dependence of $f(T)$ is influenced in a similar way by the chain length as the mean-square bond length, there are again some distinct qualitative differences between the two quantities. In the high-temperature ($T \in [0.6, 1.6]$) the mean-square bond length increases stronger (about 4%) than the amount of 180° angles (only about 0.4%). Therefore, it seems that bond vectors in the ground state do not make their adjacent bond vectors to align with them. Correlations between the orientations of subsequent bond vectors are negligible in the high-temperature region, whereas they become more important in the intermediate-temperature region between $T = 0.5$ and $T = 0.1$. Depending upon the chain length, the number of 180° angles approximately increases between 10 and 30 times stronger than in the high-temperature region, while the comparable expansion of the mean-square bond length in the interval $T \in [0.1, 0.5]$ over its value for $T \in [0.6, 1.6]$ is only a factor 3–5. Therefore, it seems that the increase of the ground-state population induces a strong stretching of the bond angle. This stretching is also visible if one looks at the temperature dependence of the mean bond angle (Figure 7). The smaller the chain length, the more the bond angle can expand over its high-temperature value, as is expected from the previous results. However, what could not be expected is that no other angle gains as much weight with

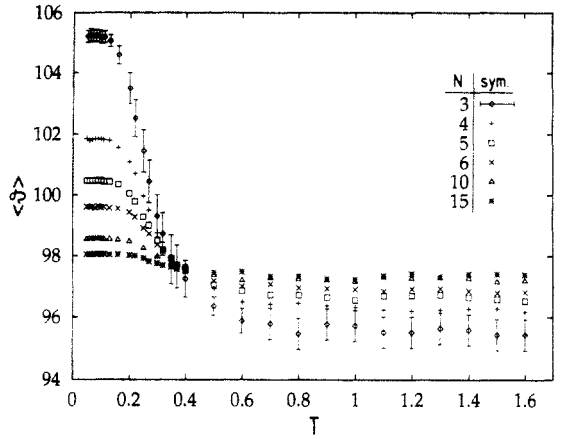

Figure 7. Plot of the mean bond angle for the same chain lengths and cooling rate as in Figure 2. Again the error bars are only shown for one chain length $N = 3$ for the sake of clearness.

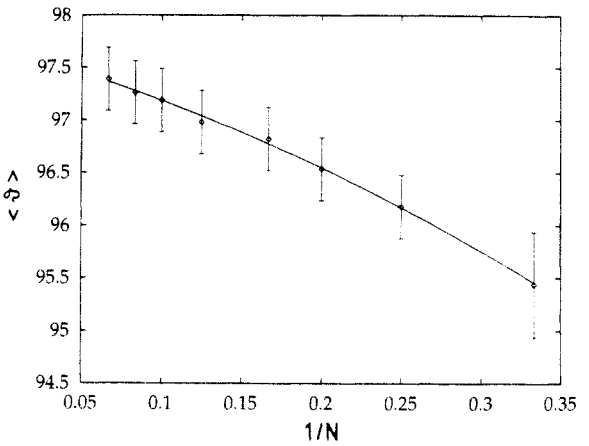

Figure 8. Variation of the mean bond angle with the inverse chain length at $T = 1.6$, taken from Figure 7. The solid line corresponds to a fit by eq 4.

decreasing temperature as the 180° angle does, although the 90° angle has the higher *a priori* probability for two adjacent bonds in the ground state. Therefore, this effect which is apparent from a comparison of the temperature dependence of the full bond angle distribution function (not shown here) may be interpreted in terms of a cooperative development of short-range static correlations as a result of the interplay between the bond energy and the density.

Contrary to the mean-square bond length, the values of the mean bond angle in the high-temperature region do not coincide for the different studied chain lengths. If one extracts this chain-length dependence by choosing the angle at $T = 1.6$ as a representative value for the thermally equilibrated melt, one obtains the result which is shown in Figure 8. For $N \geq 5$ (i.e., $1/N = 0.2$) the mean bond angle varies linearly with the inverse chain length, whereas the dependence on N is approximately quadratic for smaller chain sizes. Therefore, one can explain the influence of the chain length on the mean bond angle by the first two terms of a $1/N$ expansion, i.e.

$$\langle \vartheta \rangle(N) = A + \frac{B}{N} + \frac{C}{N^2} + \mathcal{O}\left(\frac{1}{N^3}\right) \tag{4}$$

yielding $A = 96.67 \pm 0.25$, $B = -4.09 \pm 1.51$, and $C = -7.67 \pm 2.02$ for the three fit parameters. This fit curve is shown as a solid line in Figure 8. The fact that the mean bond angle of a thermally equilibrated coarse-grained polymer depends upon the chain length was also found in an analysis of the bond angle distribution of simple bead chains.[18] For the simplest bead chain, the random walk, the bond angle distribution, and thus also the mean bond angle of a coarse-grained bead chain could analytically be determined for arbitrary chain lengths of the underlying random walk. It was found that the mean bond angle quadratically depends upon the inverse chain length in leading order.[18] The linear term vanished due to the Gaussian character of the random walk on all length scales.[5,17] Contrary to that, the linear contribution in the $1/N$ expansion to the mean bond angle is present in this simulation because the bond-fluctuation model adopts the Gaussian random-walk behavior only for $N \geq 5$.

IV. Chain-Length Dependence of the Glass Transition Temperature

From the temperature dependence of the various "S-shaped quantities", presented in the previous sections, one can determine the influence of the chain length on the glass transition temperature. To this end, T_g may be extracted from these data as the intersection point of a linear extrapolation from the liquid with that of the glassy region.[1,2,9] A glance at the plots of the last sections shows, however, that only the linear extrapolation from the glassy region is well-defined but not that from the liquid side because the choice of the optimal temperature interval for the extrapolation is not obvious. Exactly the same kind of problems were encountered in our previous study of the cooling rate effects on the glass transition in this model,[9] and it was found that the result for $T_g(\Gamma_Q)$ was sensitively influenced by the size of the available interval for the linear extrapolation in the liquid region. The expected qualitative relationship between the T_g and the cooling rate was only recovered if one uses a quantity for which the linear extrapolation from both the glassy and the liquid side can unambiguously be performed.

Such a quantity is, for instance, the internal temperature T_i of the melt.[9] Since the definition and the properties of the internal temperature are discussed in ref 9, we only summarize those details which are necessary for our subsequent analysis. As long as the melt is in thermal equilibrium, the external heat bath, characterized by the temperature T, determines the distribution of the bond vectors on the two energetic states of the Hamiltonian (1). However, the melt decouples more and more from the external heat bath during the cooling process, until it finally falls out of equilibrium and vitrifies. Then the external temperature T may be changed without affecting the population of the two energetic states. The melt possesses its own internal temperature T_i which is reflected in the actually existing distribution of the bond vectors. This distribution can thus serve as "thermometer" to measure the internal temperature of the melt if one requires T_i to be:[9]

$$T_i := \left[\frac{1}{\epsilon} \ln \frac{g_\epsilon N(0)}{g_0 N(\epsilon)}\right]^{-1} \tag{5}$$

In this equation $N(0)$, $N(\epsilon)$, g_0, and g_ϵ stand for the number of bonds in the ground and the excited state and for the degree of degeneracy of the ground and the excited state, respectively.[9] The derivation of this equation assumes that the distribution of the bond vectors on the two energy levels is exclusively determined by the Hamiltonian and thus ignores the contribution due to the density, i.e., due to the entropy of the melt. However, the entropy will certainly exert an influence on the distribution of the bond vectors, especially at high temperatures. Therefore, the quantity, defined in eq 5, should not be looked upon as an accurate estimate of the actual internal temperature

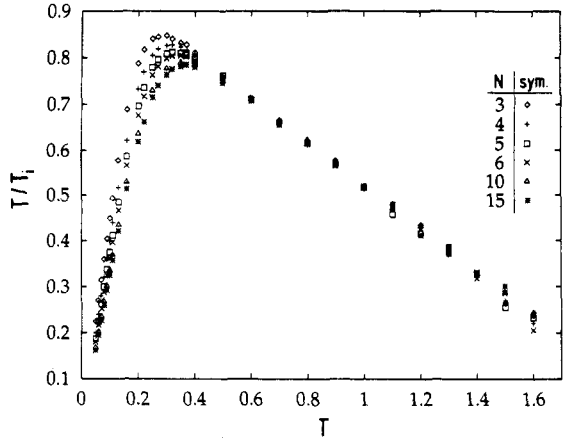

Figure 9. Plot of T/T_i vs T for the six representative chain lengths with the same choices as in Figure 2.

of the melt but rather as a first-order approximation for it. The neglect of the entropy effects in the definition of eq 5 becomes visible in Figure 9, where the temperature dependence of the ratio T/T_i is depicted. If the effects of the entropy were accurately taken into account, the internal and the external temperatures should coincide as long as the melt is in thermal equilibrium. Contrary to this expectation, one finds that the ratio T/T_i increases with a finite slope with falling temperature.

Despite this deficiency in the definition of T_i, the introduced internal temperature exhibits two interesting features. First, it can be used to scale the simulation results for different chain lengths onto one single master curve for all quantities probing the length scale of a bond since this length scale also entered the definition of the internal temperature by the distribution of the bond vectors. Such a quantity is, for instance, the specific heat per bond C_b that may be calculated either by the temperature derivative of the mean energy per bond $E_b(T)$ or by the application of the standard fluctutation relation from statistical mechanics:[19]

$$C_b := \frac{dE_b}{dT} = \frac{1}{T^2}\langle(\mathcal{H}(\vec{b}) - E_b)^2\rangle \tag{6}$$

Both ways of determining the specific heat must yield the same result as long as the melt is in thermal equilibrium. If the melt, however, falls out of equilibrium, differences may be observed. Whereas the specific heat calculated from the derivative of the energy exhibits the typical shape of a two-level system, i.e., a Schottky anomaly (not shown here), C_b from the fluctuation relation steeply increases when the melt vitrifies because the main temperature dependence then comes from the prefactor in eq 6 (i.e., $C_b \propto T^{-2}$). This explosion of the specific heat data for small temperatures can be completely removed if one replaces the prefactor in the fluctuation formula by $1/T_i^2$ and plots C_b versus the internal temperature. The result of this substitution is shown in Figure 10. Now, the specific heat data for the different chain lengths do not only exhibit a Schottky peak, but they also nicely collapse onto one single scaling curve which can accurately be described by the analytical expression of the specific heat of an isolated two-level system, i.e., for a random-walk (RW) chain, C_b^{RW}.

$$C_b^{RW} = g_0 g_\epsilon \frac{(\beta\epsilon)^2 \exp[-\beta\epsilon]}{Z_{RW}(\beta)^2} \tag{7}$$

whereby Z_{RW} is the corresponding partition function.[9]

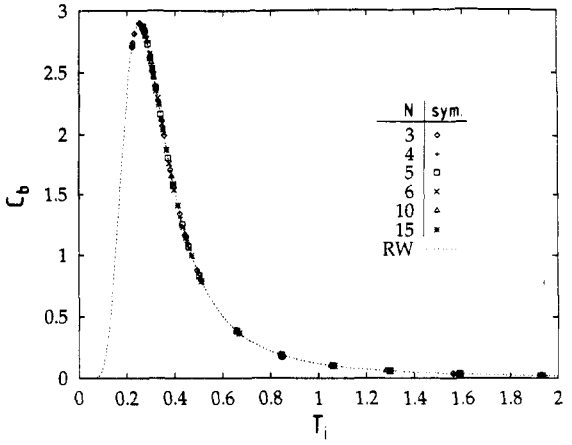

Figure 10. Plot of the specific heat vs T_i for the same chain lengths as in Figure 2. C_b was calculated by replacing T by T_i in the fluctuation relation of eq 6. The dashed curve corresponds to the random-walk approximation of C_b according to eq 7.

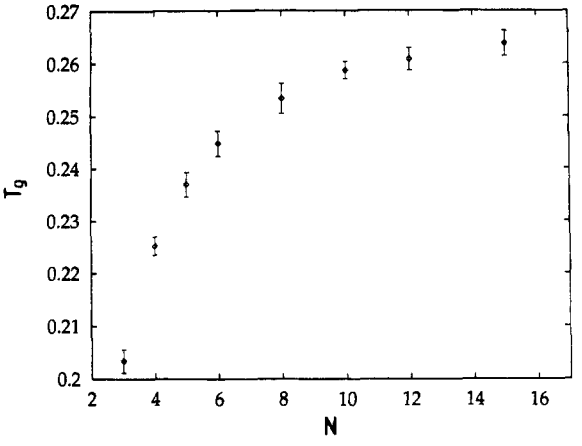

Figure 11. Plot of T_g versus N, which was determined from the internal temperature.

This result is shown as a dashed line in Figure 10. As for the cooling rate,[9] it is thus possible to reduce the complicated many-body interaction of the chains on the length scale of a bond on a single bond problem by virtue of the above defined internal temperature. The causes and further corollaries of these properties are currently under study.

The second important feature of the introduced internal temperature is that the T/T_i versus T curve of Figure 9 allows for a well-defined linear extrapolation from the liquid side so that the intersection point and thus the glass transition temperature may unambiguously be determined. The result of this analysis for the chain-length dependence of T_g is presented in Figure 11. As is usually found in experiments[20-22] and other simulations,[23] the glass transition temperature first increases strongly with N for small chain lengths (i.e., for $N \leq 6$), before its variation with N flattens more and more and seems to approach a constant value in the limit $N \to \infty$. Therefore, one expects T_g to vary asymptotically as

$$T_g(N) = T_g^\infty + A/N \tag{8}$$

which suggests to plot T_g versus $1/N$ in order to test this expectation.[20-22] For this simulation Figure 12 presents such a plot. It shows that it is indeed possible to fit the simulation data for all studied chain lengths within the error bars by eq 8. From the fit one obtains the following values for the two parameters appearing in eq 8: $T_g^\infty = 0.281 \pm 0.002$ and $A = -0.23 \pm 0.01$. Although the quality

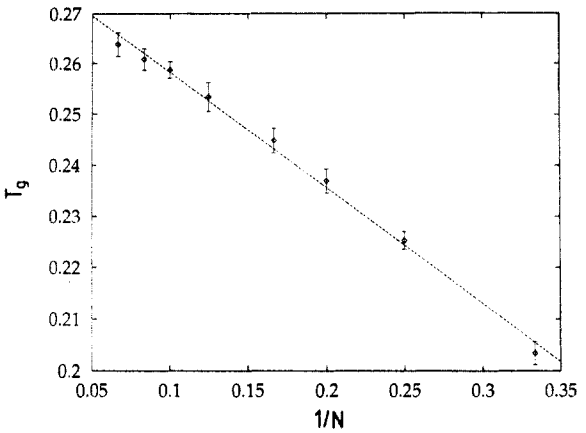

Figure 12. Plot of T_g versus $1/N$ in order to check the expected asymptotic behavior of eq 8. The dashed line is the result of a linear regression to all the data points.

of the fit is reasonably good and the fact that such a fit is feasible seems to exemplify again the influence of the chain ends on the ability of a polymer to relax, a closer inspection of Figure 12 shows that T_g vs $1/N$ data are clearly curved. Therefore, one might assume the simulation data for chains larger than those studied to fall below the determined linear relationship. Whether this is really the case could only be checked by an extension of the presented analysis to much larger chain lengths, which was beyond the computational scope of this work.

Experimental investigations of the N dependence of T_g[21,22] show that the relationship between T_g and $1/N$ should not be expected to be strictly linear over the entire range of chain lengths but rather to exhibit an inflection point separating a linear regime for small chains from another one for large chains. The regime for the large chains possesses a larger slope than that for the small chain lengths, and thus the T_g vs $1/N$ curve bends upward contrary to the curvature found in this simulation. However, one has to be careful when comparing our data to experimental work, since our chains are much shorter than the entanglement chain length N_e ($N_e \approx 30$ for athermal melts of our model[24]), whereas the inflection point in the experimental curves occurs at rather high molecular weights and thus might be related to N_e. In fact, if one assesses the molecular weight, where the linear regime for the large chains ends, from experimental data,[21,22] and compares the resulting values with the entanglement molecular weights taken from,[25] it turns out that they are rather close to each other. Although this coincidence may be accidential, the speculation that the inflection point in the T_g versus $1/N$ curve has something to do with N_e seems to be reasonable, especially if one takes the strong difference in chain-length dependence of the viscosity of a melt below and above N_e[5] and the mentioned definition of T_g by the viscosity into account.

V. Summary and Outlook

This paper provides an overview of the results for the chain-length dependence of the structural glass transition of a three-dimensional model for polymer melts. The polymers are simulated by a combination of the bond-fluctuation model with a simple two-level Hamiltonian. The interplay of this Hamiltonian with the density of the melt creates a competition between the energetic and the geometric constraints in the system, which prevents some bonds from reaching the ground state during the finite cooling time. They have to remain in the energetically unfavorable excited state. While the melt vitrifies, they are *geometrically frustrated*. The extent to which this geometric frustration is pronounced depends upon the chain length of the polymers. Since smaller chains are more mobile than larger ones, they cannot so easily be trapped in configurations from which relaxation is difficult during the finite cooling time, and thus they start to vitrify at a lower temperature than the longer chains. Due to this influence of the chain length on the ability of the polymers to relax, the glass transition temperature T_g increases with the chain length. If one determines the chain-length dependence of T_g, one finds an approximate linear relationship betwene T_g and the inverse chain length, as is also borne out in many experiments[20-22] and other computer simulations.[23] Therefore, the introduced model for the structural glass transition in polymer melts also reproduces this experimental feature in addition to many other aspects that have been studied previously.[7-10] In comparison with these previous studies, it is interesting to note that the chain length qualitatively affects the freezing behavior of the melt in a similar fashion as the cooling rate does. The smaller the chain length (cooling rate), the later the melt falls out of equilibrium. This qualitative similarity between the effects of the chain length and the cooling rate may be exemplified by calculation of the specific heat per bond. If one calculates the specific heat according to the standard fluctuation relation of statistical mechanics, it strongly increases with falling temperature due to the prefactor $1/T^2$. Replacing the external temperature in this prefactor by the internal temperature and plotting the specific heat versus T_i instead of versus T, one succeeds in scaling the simulation data for all studied chain lengths onto one single master curve which coincides with the master curve stemming from a variation of the cooling rate. Therefore, this result seems to indicate that time and length scales, at least along the chains, are connected with each other.

Starting from the results presented in this work, we want to extend our study by repeating the analysis for a two-dimensional polymer melt. Keeping all other external control parameters fixed, a comparison between the two- and the three-dimensional results should yield some insight in the influence of the spatial dimension on the glass transition in this model. Such an influence of the spatial dimension on the properties close to the transition is well-known from the systems undergoing a second-order phase transition[26] or possessing quenched disorder.[27,28] Although the structural glass transition certainly has a different origin than a second-order phase transition, the question about the influence of the spatial dimension on it is nevertheless very interesting from a theoretical point of view and has not been paid much attention to yet.

Acknowledgment. We are very grateful to the Höchstleistungsrechenzentrum (HLRZ) at Jülich, to the Regionales Hochschulrechenzentrum Kaiserslautern (RHRK), and to the Zentrum für elektronische Datenverarbeitung at Mainz for a generous grant of computer time on the CRAY-YMP, on the VP100, and on a UNIV-workstation cluster and to the Deutsche Forschungsgemeinschaft for support (SFB 262).

References and Notes

(1) Jäckle, J. *Rep. Prog. Phys.* **1986**, *49*, 171.
(2) Zallen, Z. *The Physics of Amorphous Solids*; Wiley: New York, 1983.
(3) Eisele, U. *Introduction to Polymer Physics*; Springer: Heidelberg, 1990.
(4) Kremer, K.; Binder, K. *Comput. Phys. Rep.* **1988**, *7*, 259.

(5) Doi, M.; Edwards, S. F. *Theory of Polymer Dynamics*; Clarendon Press: Oxford, U.K., 1986.
(6) Carmesin, I.; Kremer, K. *Macromolecules* **1988**, *21*, 2819. Deutsch, H.-P.; Binder, K. *J. Chem. Phys.* **1991**, *94*, 2294. Wittmann, H.-P.; Kremer, K. *Comput. Phys. Commun.* **1990**, *61*, 309. Wittmann, H.-P.; Kremer, K. *Comput. Phys. Commun.* **1992**, *71*, 343.
(7) Paul, W.; Baschnagel, J. In *Monte Carlo and Molecular Dynamics Simulations in Polymer Science*; Binder, K., Ed.; Oxford University Press: New York, in press.
(8) Baschnagel, J.; Wittmann, H.-P.; Paul, W.; Binder, K. In *Trends in Non-Crystalline Solids*; Conde, A., Conde, C. F., Millán, M., Eds.; World Scientific: Singapore, 1992.
(9) Baschnagel, J.; Binder, K.; Wittmann, H.-P. *J. Phys. C: Condens. Matter* **1993**, *5*, 1597.
(10) Baschnagel, J.; Binder, K. *Physica A* **1994**, *204*, 47.
(11) Brüning, R.; Samwer, K. *Phys. Rev. B* **1992**, *46*, 11318.
(12) The temperature and all energies are measured in units of ϵ. All length and time scales are measured in units of lattice constants and of Monte Carlo steps, respectively. Arguments have been presented that one lattice constant and a Monte Carlo step physically correspond to a length of about 2 Å and to a time of about 10^{-13} s.[7]
(13) Binder, K.; Heermann, D. W. *Monte Carlo Simulation in Statistical Physics: An Introduction*; Springer: Heidelberg, 1992.
(14) Gény, F.; Monnerie, L. *J. Polym. Sci.* **1979**, *17*, 147.
(15) Kolinksi, A.; Skolnick, J.; Yaris, R. *J. Chem. Phys.* **1986**, *84*, 1922.
(16) Baschnagel, J.; Binder, K.; Paul, W.; Laso, M.; Suter, U. W.; Batoulis, I.; Jilge, W.; Bürger, T. *J. Chem. Phys.* **1991**, *95*, 6014. Baschnagel, J.; Qin, K.; Paul, W.; Binder, K. *Macromolecules* **1992**, *25*, 3117.
(17) Flory, P. J. *Statistical Mechanics of Chain Molecules*; Wiley: New York, 1969.
(18) Laso, M.; Oettinger, H. C.; Suter, U. W. *J. Chem. Phys.* **1991**, *95*, 2178.
(19) Huang, K. *Statistical Mechanics*; Wiley: New York, 1963.
(20) Fox, T. B.; Loshaek, S. *J. Polym. Sci.* **1955**, *15*, 371. Fox, T. G.; Flory, P. J. *J. Polym. Sci.* **1954**, *14*, 315.
(21) Rubin, A.; Burgin, D. *Polymer* **1975**, *16*, 291. Pezzina, G.; Zilio-Grandi, F.; Saumartin, P. *Eur. Polym. J.* **1970**, *6*, 1053. Cowie, J. M.; Toporowski, P. M. *Eur. Polym. J.* **1968**, *4*, 621.
(22) McKenna, G. B. In *Comprehensive Polymer Science*; Booth, C., Price, C., Eds.; Pergamon Press: New York, 1989; Vol. 2.
(23) Roe, R.-J.; Rigby, D.; Furuya, H.; Takeuchi, H. *Comput. Polym. Sci.* **1992**, *2*, 32.
(24) Paul, W.; Binder, K.; Heermann, D. W.; Kremer, K. *J. Chem. Phys.* **1991**, *95*, 7726. Paul, W.; Binder, K.; Heermann, D. W.; Kremer, K. *J. Phys. II* **1991**, *1*, 37.
(25) Wool, R. P. *Macromolecules* **1993**, *26*, 1564.
(26) Stanley, H. E. *Introduction to Phase Transitions and Critical Phenomena*; Oxford University Press: New York, 1987.
(27) Binder, K.; Young, A. P. *Rev. Mod. Phys.* **1986**, *58*, 801.
(28) Binder, K.; Reger, J. D. *Adv. Phys.* **1992**, *41*, 547.